第38卷第6期 无 机 化 学 学 报 Vol.38 No.6
2022年6月 CHINESE JOURNAL OF INORGANIC CHEMISTRY 1171-1179

四个基于间苯二(取代水杨醛酰腙)的有机锡配合物的溶剂热合成、结构和荧光性能

冯泳兰 蒋伍玖 张复兴 邝代治*
(功能金属有机化合物湖南省重点实验室,金属有机新材料湖南省高校重点实验室,
衡阳师范学院化学与材料科学学院,衡阳 421008)

摘要: 采用间苯二(取代水杨醛酰腙)(H_4L)与R^2_3SnOH溶剂热反应,或间苯二甲酰肼、3-叔丁基水杨醛和三环己基氢氧化锡一锅溶剂热法反应,合成了4个新的有机锡配合物$(SnR^2)_2L$ (**1~4**),其中,H_4L=*m*-Ph(CONH—N=CH(*o*-OH)PhR^1)$_2$;R^1=NEt_2,R^2=Ph (**1**);R^1=3,5-di-*tert*-butyl=3,5-*t*-2Bu,R^2=Ph (**2**);R^1=3,5-*t*-2Bu,R^2=Cy (**3**);R^1=3-*tert*-butyl=3-*t*-Bu,R^2=Cy (**4**)。经元素分析、红外光谱和(^{1}H、^{13}C、^{119}Sn)核磁共振谱表征,并用X射线衍射方法确证配合物**1~4**的结构。配体H_4L的2个取代水杨醛酰腙链向内取向并与锡原子配位形成3个内向*E*型配合物**1~3**,取代水杨醛酰腙链向外取向并与锡原子配位形成外向*E*型配合物**4**。配合物**1**、**2**和**4**属于三斜晶系$P\bar{1}$空间群,配合物**3**属于单斜晶系$P2_1/c$空间群。中心锡与配位原子构成畸形双角三锥构型。配体、配合物-三氯甲烷溶液的荧光性能表明,当具有弱荧光的配体*m*-Ph(CONH—N=CH(*o*-OH)PhNEt_2)$_2$(H_4L^1)和无荧光的配体*m*-Ph(CONH—N=CH(*o*-OH)Ph(3,5-*t*-2Bu))$_2$(H_4L^2)分别与苯基锡、环己基锡配位后,配合物-三氯甲烷溶液发出强荧光。

关键词: 间苯二(取代水杨醛酰腙);有机锡配合物;溶剂热合成;晶体结构;荧光性质
中图分类号: O614.43$^+$2 **文献标识码:** A **文章编号:** 1001-4861(2022)06-1171-09
DOI: 10.11862/CJIC.2022.105

Solvothermal Synthesis, Structure, and Fluorescence Properties of Four Organotin Complexes Based on *m*-Phthaloyl Bis(substituted salicylaldehyde acylhydrazone)

FENG Yong-Lan JIANG Wu-Jiu ZHANG Fu-Xing KUANG Dai-Zhi*
(*Key Laboratory of Functional Metal-Organic Compounds of Hunan Province, Key Laboratory of Organometallic New Materials of College of Hunan Province, College of Chemistry and Material Science, Hengyang Normal University, Hengyang, Hunan* 421008, *China*)

Abstract: Four new organotin complexes based on *m*-phthaloyl bis(substituted salicylaldehyde acylhydrazone) (H_4L), $(SnR^2)_2L$ (**1-4**), were synthesized by solvothermal reaction of H_4L with R^2_3SnOH, or one-pot solvothermal reaction of *m*-phthaloyl hydrazide, 3-*tert*-butyl salicylaldehyde, and tricyclohexyltin hydroxide, where H_4L=*m*-Ph(CONH—N=CH(*o*-OH)PhR^1)$_2$; R^1=NEt_2, R^2=Ph (**1**); R^1=3,5-di-*tert*-butyl=3,5-*t*-2Bu, R^2=Ph (**2**); R^1=3,5-*t*-2Bu, R^2=Cy (**3**); R^1=3-*tert*-butyl=3-*t*-Bu, R^2=Cy (**4**). And they were characterized by elemental analysis, IR, and (^{1}H, ^{13}C, and ^{119}Sn) NMR. The structures of complexes **1-4** were confirmed by X-ray diffraction. Three "inward *E*-type" complexes **1-3** were formed by the inward orientation of two substituted salicylaldehyde acylhydrazone chains of H_4L and coordination with tin atoms. And two substituted salicylaldehyde acylhydrazone chains were oriented outward and coordinated with tin atoms to form an "outward *E*-type" complex **4**. Complexes **1**, **2**, and **4** belong to the triclinic $P\bar{1}$ space group and complex **3** belongs to the monoclinic $P2_1/c$ space group. The central tin and the coordination atom form a five-coordinate distorted triangular bipyramids configuration. The fluorescence properties of the ligands and the

收稿日期:2021-12-18。收修改稿日期:2022-03-11。
功能金属有机化合物湖南省重点实验室资助。
*通信联系人。E-mail:hnkcq@qq.com

complexes-chloroform solution showed that when free ligand *m*-Ph(CONH—N=CH(*o*-OH)PhNEt$_2$)$_2$ (H_4L^1) with weak fluorescence and ligand *m*-Ph(CONH—N=CH(*o*-OH)Ph(3,5-*t*-2Bu))$_2$ (H_4L^2) without fluorescence coordinated with phenyltin or cyclohexyltin, the chloroform solution of the complexes emitted strong fluorescence. CCDC: 2111478, **1**; 2111479, **2**; 2111480, **3**; 2111481, **4**.

Keywords: *m*-phthaloyl bis(substituted salicylaldehyde acylhydrazone); organotin complex; solvothermal synthesis; crystal structure; fluorescence properties

0 Introduction

Nucleophilic addition and dehydration of organic aldehydes or ketones with hydrazide result in acylhydrazone compounds containing amide Schiff base ($R^1C(O)$—NH—N=CH(R)—R^2). The acylhydrazone compounds not only have good bactericidal[1-2], antitumor[3-4], and optical properties[5-9] but also provide multiple coordination atoms such as oxygen and nitrogen. These —CH=N—, >NH and —CONH— active groups have their respective chemical reactivity and cooperation interaction effect. The lone pair electrons of amino-group (>NH) are p-π conjugated with adjacent carbonyl and double bond imine-groups, and the double bond produces *Z*-, *E*-isomerization[10]. Therefore, acylhydrazone compounds have a variety of coordination modes with metals, providing a broad space for the synthesis of complexes with diverse structures and functions[11-13]. Therefore, people are inspired to think that acylhydrazone compounds[14-15] containing bis(poly)-acylhydrazone X[NH—N=CHAr(OH)]$_2$ (X can be carbonyl >C=O/S, aromatic polycarbonyl, and other bridge groups or atoms) have more active groups, more coordination modes than monoacylhydrazone, and are more prone to keto and enol conversion of acylhydrazone chain and deprotonation of amide nitrogen[16]. The coordination of acylhydrazone compounds with metals to assemble complexes with various structures and properties[17] has attracted more interest. In this work, *m*-phthaloyl bis(substituted salicylaldehyde acylhydrazone) compounds (H_4L) were prepared by condensation of 4-diethylaminosalicylaldehyde, 3,5-di-*tert*-butyl salicylaldehyde and 3-*tert*-butyl salicylaldehyde with *m*-phthaloyl hydrazine, respectively. The triphenyltin hydroxide and tricyclohexyltin hydroxide reacted with H_4L respectively to synthesize organotin diacylhydrazone complexes ($SnR^2)_2L$ (**1**-**4**), where H_4L=*m*-Ph(CONH—N=CH(*o*-OH)PhR^1)$_2$; R^1=NEt_2, R^2=Ph (**1**); R^1=3,5-di-*tert*-butyl=3,5-*t*-2Bu, R^2=Ph (**2**); R^1=3,5-*t*-2Bu, R^2=Cy (**3**); R^1=3-*tert*-butyl=3-*t*-Bu, R^2=Cy (**4**). The fluorescence properties of the complexes were preliminarily evaluated.

1 Experimental

1.1 Material and instruments

FT-IR spectra were recorded on a Bruker TENSOR Ⅱ Fourier infrared spectrometer with the samples prepared as KBr (400-4 000 cm^{-1}) pellets. C, H, and N analyses were carried out with a PE-2400 Ⅱ element analyzer. UV-Vis absorption spectra were recorded on a UV-2500PC spectrophotometer. ^{1}H, ^{13}C, and ^{119}Sn NMR spectra were determined by Bruker Avance 500 NMR (TMS as internal standard and $CDCl_3$ or DMSO-d_6 as solvent). Melting points were measured by an X-4 microscopic melting point apparatus made by Beijing Tech Instrument Co., Ltd. and were uncorrected. Fluorescence spectra in the solution were recorded on a Hitachi F-7000 spectrometer.

4-Diethylaminosalicylaldehyde(99%) and 3-*tert*-butyl salicylaldehyde (CP) (Beijing, J&K Chemical Ltd.), *m*-phthaloyl hydrazide and 3,5-di-*tert*-butyl salicylaldehyde (CP) (Shanghai Shaoyuan Co., Ltd.), tricyclohexyltin hydroxide (CP) (Hubei Jusheng Technology Co., Ltd.), triphenyltin hydroxide (CP) (Shanghai Civi Chemical Technology Co., Ltd.) were used without further purification.

1.2 Preparation of the ligands

A mixture of *m*-phthaloyl hydrazide (3.890 g, 0.020 mol), 4-diethylaminosalicylaldehyde (7.732 g, 0.040 mol), and 60 mL ethanol solution was placed in a flask. The reactant was stirred and refluxed until the

solid was dissolved, and the reaction continued for 24 h. Then the mixture was cooled and filtered. The obtained solid was recrystallized and dried in a vacuum to obtain 8.420 g of orange powder of *m*-phthaloyl bis (4-diethylaminosalicylaldehyde acylhydrazone) (H_4L^1), with a yield of 75.0%. m.p. 300 ℃. Anal. Calcd. for $C_{30}H_{36}N_6O_4$(%): C, 66.16; H, 6.66; N, 15.43. Found(%): C, 66.20; H, 6.68; N, 15.38. FT-IR (KBr, cm^{-1}): 3 448 (m, $\nu_{O—H}$); 3 292, 3 239(m, $\nu_{N—H}$); 3 072, 2 972, 2 930, 2 900(m, $\nu_{Ar—H}$ and $\nu_{C—H}$); 1 648, 1 628(vs, $\nu_{C=O}$ and $\nu_{C=N}$); 1 585, 1 546 (m, benzene $\nu_{C=C}$). ^{1}H NMR (500 MHz, DMSO-d_6): δ 12.02(s, 2H), 11.47(s, 2H), 8.50-6.15(m, 12H), 3.36(m, 8H), 1.13(s, 12H). ^{13}C NMR (126 MHz, DMSO-d_6): δ 162.14, 160.24(**C**=O); 150.71 (**C**=N); 133.99, 132.11, 131.01, 129.28, 127.17, 106.89, 104.17, 97.95 (spectral line of benzene carbon); 44.30, 40.48, 40.40, 40.31, 40.23, 40.15, 39.98, 39.81, 39.64, 39.48 (methylene carbon spectral line of ethylamine); 13.00 (methyl carbon of ethylamine).

m-Phthaloyl hydrazide (5.825 g, 0.030 mol), 3,5-di-*tert*-butyl salicylaldehyde (14.059 g, 0.060 mol) and 50 mL of ethanol were added into the reaction flask. The reactant was stirred and refluxed for 48 h. Then the mixture was cooled and filter. The precipitate was dried in a vacuum. The yellow powder (8.961 g) of *m*-phthaloyl bis(3,5-di-*tert*-butyl salicylaldehyde acylhydrazone) (H_4L^2) was obtained, with a yield of 69.1%. m.p. 114 ℃. Anal. Calcd. for $C_{38}H_{50}N_4O_4$(%): C, 72.81; H, 8.04; N, 8.94. Found(%): C, 72.85; H, 8.08;N, 8.76. FT-IR(KBr, cm^{-1}): 3 476(m, $\nu_{O—H}$); 3 252(m, $\nu_{N—H}$); 3 062, 2 960, 2 909, 2 870(m, $\nu_{Ar—H}$ and $\nu_{C—H}$); 1 669, 1 646(vs, $\nu_{C=O}$ and $\nu_{C=N}$); 1 622, 1 589 (m, benzene $\nu_{C=C}$). ^{1}H NMR (500 MHz, $CDCl_3$): δ 11.91(s, 2H), 8.76 (s, 2H), 7.46-7.01(m, 10H), 1.57-1.20(m, 36H). ^{13}C NMR (126 MHz): δ 165.29(**C**=O); 156.86(**C**=N); 141.29, 136.88, 128.24, 126.98, 116.70 (spectral line of benzene carbon); 35.15, 34.21, 31.45, 29.45 (*tert*-butyl carbon).

1.3 Synthesis of the complexes

H_4L^1 (0.545 g, 1 mmol), triphenyltin hydroxide (0.734 g, 2 mmol), and 8 mL mixed solvent (3 mL methanol and 5 mL DMF) were mixed and heated to 120 ℃ for 72 h, then the mixture was reduced to room temperature at 1 ℃·h^{-1} and filtered. Complex **1** was obtained by recrystallization.

Complex **2** was synthesized by replacing H_4L^1 with H_4L^2 (0.433 g, 1 mmol). Complex **3** was synthesized by replacing triphenyltin hydroxide with tricyclohexyltin hydroxide and reacting with H_4L^2.

One-pot solvothermal synthesis of complex **4**: *m*-phthaloyl hydrazide (0.194 g, 1 mmol), 3-*tert*-butyl salicylaldehyde (0.356 g, 2 mmol), tricyclohexyltin hydroxide (0.771 g, 2 mmol) and 8 mL methanol were added to the polytetrafluoroethylene reactor. Then, following the synthesis steps of complex **1**, complex **4** was obtained.

Complex **1**, orange crystal, 0.869 g, Yield: 80.0%. m.p. 300 ℃. Anal. Calcd. for $C_{54}H_{52}N_6O_4Sn_2$(%): C, 59.70; H, 4.82: N, 7.74. Found(%): C, 60.01; H, 4.78: N, 7.71. FT-IR (KBr, cm^{-1}): 3 065, 3 047, 2 971, 2 928, 2 902, 2 809(m, $\nu_{Ar—H}$ and $\nu_{C—H}$); 1 607, 1 586(s, $\nu_{C=O}$ and $\nu_{C=N}$); 1 505, 1 479 (m, benzene $\nu_{C=C}$); 546(w, $\nu_{Sn—O}$); 500(w, $\nu_{Sn—N}$); 451(w, $\nu_{Sn—C}$). ^{1}H NMR (500 MHz, $CDCl_3$): δ 8.97(s, 2H), 8.57-6.16(m, 10H) 3.40(m, 8H), 1.25(s, 12H). ^{13}C NMR (126 MHz, $CDCl_3$): δ 169.16, 166.57(**C**=O); 160.05, 153.87(**C**=N); 140.02, 136.57, 136.40, 136.35, 136.14, 133.99, 130.12, 129.38, 129.00, 128.67, 128.32, 128.02, 126.30, 107.18, 103.99, 100.98 (carbon of benzene); 44.63 (methylene carbon of ethylamino); 12.86 (methyl carbon of ethylamino). ^{119}Sn NMR ($SnMe_4$, 187 MHz, $CDCl_3$): δ −329.62.

Complex **2**, orange red crystal, 0.594 g, Yield: 50.8%. m.p. 253-255 ℃. Anal. Calcd. for $C_{62}H_{67}N_4O_4Sn_2$ (%): C,63.72; H, 5.69; N, 4.79. Found(%): C, 63.68; H, 5.75; N, 4.75. FT-IR (KBr, cm^{-1}): 3 059, 2 959, 2 906, 2867(s, $\nu_{Ar—H}$ and $\nu_{C—H}$); 1 611, 1 591(s, $\nu_{C=O}$ and $\nu_{C=N}$); 1 552, 1 537, 1 509, 1 477, 1 460 (m, benzene $\nu_{C=C}$); 694(w, $\nu_{Sn—O}$); 443(w, $\nu_{Sn—N}$); 407(w, $\nu_{Sn—C}$). ^{1}H NMR (500 MHz, $CDCl_3$): δ 9.00, 8.87(s, 2H), 8.75-7.02(m, 30H), 1.53, 1.47, 1.32(m, 36H). ^{13}C NMR (126 MHz, $CDCl_3$): δ 168.46, 165.27, 164.94, 163.11(**C**=O); 156.86 (**C**=N); 141.29, 140.58, 139.63, 139.21, 137.95, 137.24, 136.89, 136.46, 136.24, 136.14, 136.02, 133.53, 131.03, 130.35, 130.31, 129.13, 128.96, 128.79, 128.64, 128.44, 128.33, 128.22, 127.02, 126.97, 116.71, 116.29 (carbon of benzene); 35.48, 35.14, 34.19, 34.03, 31.44, 31.29, 30.09, 29.46 (carbon of *tert*-butyl). ^{119}Sn NMR ($SnMe_4$,

187 MHz, $CDCl_3$): δ −324.04.

Complex **3**, orange flake crystal, 0.476 g, Yield: 39.9%. m. p. 278 ℃. Anal. Calcd. for $C_{62}H_{92}N_4O_4Sn_2$ (%): C, 62.32; H, 7.76; N, 4.69. Found(%): C, 62.45;H, 7.78; N, 4.65. FT-IR (KBr, cm^{-1}): 3 014, 2 950, 2 920, 2 848 (s, $\nu_{Ar—H}$ and $\nu_{C—H}$); 1 611, 1 595(s, $\nu_{C=O}$ and $\nu_{C=N}$); 1 548, 1 534, 1 518 (m, benzene $\nu_{C=C}$); 525(w, $\nu_{Sn—O}$); 484(w, $\nu_{Sn—N}$); 459(w, $\nu_{Sn—C}$). ^{1}H NMR (500 MHz, $CDCl_3$): δ 9.07-8.63(m, 2H), 8.19-6.81(m, 8H), 1.96-1.30(m, 80H). ^{13}C NMR (126 MHz, $CDCl_3$): δ 168.89, 165.35, 162.47(**C**═O); 156.86(**C**═N); 140.07, 137.93, 133.98, 130.28, 129.87, 128.53, 128.02, 126.67, 116.08 (carbon of benzene); 39.94, 35.29, 33.95, 31.35, 31.13, 29.93, 29.91, 29.69, 28.82, 28.55, 28.53, 26.76, 26.61 (carbon of *tert*-butyl and cyclohexyl). ^{119}Sn NMR ($SnMe_4$, 187 MHz, $CDCl_3$): δ −249.76.

Complex **4**, yellow block crystal, 0.26 g, Yield: 24.1%. m. p. 226 ℃. Anal. Calcd. for $C_{54}H_{74}N_4O_4Sn_2$ (%): C, 60.02; H, 6.90; N, 5.18. Found(%): C, 60.05; H, 6.92: N, 5.11. FT-IR (KBr, cm^{-1}): 3 053, 3 017, 2 996 (s, $\nu_{Ar—H}$ and $\nu_{C—H}$); 1 606(s, $\nu_{C=O}$ and $\nu_{C=N}$); 1 547, 1 516, 1 443(m, benzene $\nu_{C=C}$); 534(w, $\nu_{Sn—O}$); 497(w, $\nu_{Sn—N}$); 455(w, $\nu_{Sn—C}$). ^{1}H NMR (500 MHz, $CDCl_3$): δ 8.79(m, 2H), 8.19-6.68(m, 10H), 2.13-1.21(m, 62H). ^{13}C NMR (126 MHz, $CDCl_3$): δ 168.46, 165.27, 164.94, 163.11 (**C**═O); 156.86, 141.29, 140.58, 139.63, 139.21, 137.95, 137.24, 136.89, 136.46, 136.24, 136.14, 136.02, 133.53, 131.03, 130.35, 130.31, 129.13, 128.96, 128.79, 128.64, 128.44, 128.33, 128.22, 127.02, 126.97, 116.71, 116.29 (carbon of benzene); 35.48, 35.14, 34.19, 34.03, 31.44, 31.29, 30.09, 29.46 (carbon of *tert*-butyl and cyclohexyl). ^{119}Sn NMR ($SnMe_4$, 187 MHz, $CDCl_3$): δ −250.68.

1.4 X-ray data collection and refinement

The suitable crystals of the complexes were obtained by slow volatilization of methanol solvent. The single crystals of the complexes were mounted on a glass capillary of a Bruker SMART APEX Ⅱ CCD X-ray diffractometer. Intensity data for the crystals were measured on a diffractometer with graphite-monochromatized Mo *Kα* radiation (λ=0.071 073 nm) by using the φ-ω scan technique and a certain θ range. Multi-scan absorption correction was applied to the intensity data using the SAINT program. The structures were solved and refined by OLEX2 software[18] and SHELXS[19] program. All non-hydrogen atoms and their anisotropic thermal parameters were refined to convergence by the full-matrix least square method with the SHELXL program. Complexes **2** and **3** have a disorder of *tert*-butyl and cyclohexyl groups, respectively. After splitting and restraint, a chemically reasonable structural model and atomic displacement parameters were obtained. All hydrogen atoms were positioned geometrically and refined using a riding model. Details of the crystal data and structure refinement parameters for **1**-**4** are summarized in Table 1.

CCDC: 2111478, **1**; 2111479, **2**; 2111480, **3**; 2111481, **4**.

Table 1 Crystal data and structure refinement for complexes 1-4

Parameter	1	2	3	4
Empirical formula	$C_{54}H_{52}N_6O_4Sn_2$	$C_{62}H_{66}N_4O_4Sn_2$	$C_{62}H_{92}N_4O_4Sn_2$	$C_{54}H_{74}N_4O_4Sn_2$
Formula weight	1 086.39	1 168.70	1 194.77	1 080.55
Temperature / K	296.15	296.15	296.15	296.15
Crystal system	Triclinic	Triclinic	Monoclinic	Triclinic
Space group	$P\bar{1}$	$P\bar{1}$	$P2_1/c$	$P\bar{1}$
a / nm	1.018 44(7)	0.928 60(5)	2.121 75(13)	0.830 4(14)
b / nm	1.384 59(9)	1.445 83(8)	1.019 40(6)	1.749(3)
c / nm	1.854 86(12)	2.245 08(13)	2.885 28(17)	1.769(3)
α / (°)	74.457 0(10)	99.703 0(10)		86.64(3)
β / (°)	84.644 0(10)	90.020 0(10)	92.824 0(10)	79.44(2)
γ / (°)	89.875 0(10)	91.683 0(10)		78.39(2)
V / nm^3	2.508 2(3)	2.969 8(3)	6.233 0(6)	2.473(7)
Z	2	2	4	2

Continued Table 1

D_c / (Mg·m^{-3})	1.438	1.308	1.273	1.451
μ / mm^{-1}	1.046	0.888	0.847	1.059
F(000)	1 100.0	1 198.0	2 496.0	1 116.0
Crystal size / mm	0.23×0.2×0.18	0.14×0.14×0.12	0.22×0.2×0.15	0.15×0.12×0.12
θ range/ (°)	2.141-25.749	2.375-25.478	2.217-25.719	2.343-25.098
Limiting indices (h, k, l)	−12-12, −16-16, −22-22	−11-11, −17-16, −27-27	−25-25, −12-12, −35-35	−9-9, −20-20, −21-21
Reflection collected	27 617	32 238	66 746	25 880
Unique reflection (R_{int})	9 531 (0.016 3)	10 970 (0.019 0)	11 869 (0.031 6)	8 752 (0.020 8)
Completeness to θ / %	99.7	99.6	99.8	99.5
Data, restraint, parameter	9 531, 156, 595	10 970, 1 671, 720	11 869, 2 865, 896	8 752, 24, 559
Goodness-of-fit on F^2	1.024	1.049	1.020	1.090
Final R indices [I>2σ(I)]	R_1=0.039 3, wR_2=0.103 8	R_1=0.036 3, wR_2=0.089 9	R_1=0.074 1, wR_2=0.214 4	R_1=0.037 0, wR_2=0.098 1
R indices (all data)	R_1=0.045 7, wR_2=0.110 6	R_1=0.045 5, wR_2=0.097 3	R_1=0.094 4, wR_2=0.238 5	R_1=0.046 1, wR_2=0.104 8
Largest diff. peak and hole / (e·nm^{-3})	1 220 and −1 560	760 and −970	1 220 and −1 010	1 340 and −740

2 Results and discussion

2.1 Crystal structure of complexes

The ligands, *m*-phthaloyl bis(substituted salicylaldehyde acylhydrazone) with diacylhydrazone chains contain multiple nitrogen and oxygen atoms that can coordinate with metals. Due to the double bond C═N, the arrangement of phenyl and acyl hydrazone chains produces *E*-, *Z*-isomerism. In solids, due to hydrogen bonding, it often exists in an *E*-type configuration[20-21], In addition, the acylhydrazone chain contains a rotatable single bond. The C1—N—N═CPh(OH) and C8—N—N═CPh(OH) chains on the central benzene ring can be oriented inward and outward by C1—C2 or C4—C8 bond rotation. Theoretical calculations show that the coplanar structure of benzene and acylhydrazone chain of ligands H_4L^1 and H_4L^2 is assumed as the initial conformation (α=0°) and the C1—C2 bond rotates 360° around space. Other configurations remain unchanged, and the system energy (E) changes with the rotation (α) was explored. The difference between the maximum energy barrier and the lowest energy conformation of the curve was found ($\Delta E=E_{max}-E_{min}$) to be 20.15 kJ (H_4L^1) and 19.78 kJ (H_4L^2) respectively. It can be seen that the C1—C2 bond of H_4L^1 and H_4L^2 can rotate freely, and the two acylhydrazone chains of the ligand can coordinate with the metal in an inward orientation or outward orientation to construct mono-, poly-metal complexes. X-ray crystal structure analysis shows that complexes **1**-**3** form an *E*-type internal orientation coordination structure. In complex **4**, the C1—C2 and C4—C8 bond rotate, the configuration of the benzoylacylhydrazone chain is reversed, and the ligand atom coordinates with cyclohextin to form an *E*-type outward orientation structure. The selected bond length and bond angle data are shown in Table 2 and the molecular structure is shown in Fig.1. Complexes **1**, **2**, and **4** belong to the triclinic $P\bar{1}$ space group and complex **3** belongs to the monoclinic $P2_1/c$ space group. These two kinds of internally and externally oriented coordination structures are produced by nitrogen, oxygen from ligand with tin, which coordinate with diphenyl (dicyclohexyl) tin to construct five coordinated diphenyl (dicyclohexyl) tin complexes, in which C1—O1 and C8—O2 bonds are 0.130 1(4) and 0.130 4(4) nm, respectively, and the bond length is between the normal carbon-oxygen single bond length (0.143 0 nm) and double bond length (0.122 4 nm)[22], indicating that the carbonyl group becomes enol type. Two phenyl groups(cyclohexyl) extend up and down the ligand

"plane" to form ∠C—Sn—C: 119.39(15)° (**1**), 115.98(15)° (**2**), 134.7(6)° (**3**), and 127.97(16)° (**4**). It can be seen that cyclohexyl has a greater steric effect than phenyl. The bond parameters of the covalent bond composed of central tin and the nitrogen, oxygen, and carbon atoms of the ligand are different. O1 and O3 atoms are in the axial position at the top of the triangular bipyramid, the axial angles (∠O1—Sn1—O3) are 153°-159°, which deviates from the linear structure, and the cyclohexyltin of **3** and **4** deviates 180° more

Table 2 Selected bond lengths (nm) and bond angles (°) of complexes 1-4

Length or angle*	1	2	3	4
Sn1—O1	0.214 2(3)	0.214 4(2)	0.215 6(5)	0.210 4(3)
Sn1—O3	0.208 0(3)	0.208 1(2)	0.210 4(5)	0.204 3(4)
Sn1—Ny	0.212 4(3)	0.215 4(3)	0.214 7(5)	0.214 6(4)
Sn1—Cx_1	0.211 7(4)	0.211 8(4)	0.209 0(13)	0.211 7(5)
Sn1—Cx_2	0.212 4(4)	0.212 7(4)	0.220 6(16)	0.213 7(5)
O1—Sn1—O3	158.83(11)	155.03(10)	153.72(19)	153.76(11)
O1—Sn1—Ny	73.80(10)	73.18(9)	72.58(17)	71.81(15)
O1—Sn1—Cx_1	94.76(15)	94.38(13)	93.6(5)	97.50(17)
O1—Sn1—Cx_2	95.25(14)	94.77(13)	97.2(4)	98.05(18)
Ny—Sn1—O3	85.03(11)	83.00(9)	82.29(18)	82.73(14)
Ny—Sn1—Cx_1	119.63(14)	130.95(12)	118.1(4)	110.30(18)
Ny—Sn1—Cx_2	120.58(14)	112.30(13)	107.1(5)	121.73(17)
O3—Sn1—Cx_1	95.98(15)	95.65(13)	91.5(5)	97.18(15)
O3—Sn1—Cx_2	95.29(15)	101.22(14)	97.4(4)	89.83(17)
Cx_1—Sn1—Cx_2	119.39(15)	115.98(15)	134.7(6)	127.97(16)

* x_1=31, x2=37, y=1 for **1**; x_1=39, x_2=45, y=1 for **2**; x_1=39a, x_2=45a, y=2, Sn1=Sn1a for **3**; x_1=31, x_2=37, y=2 for **4**.

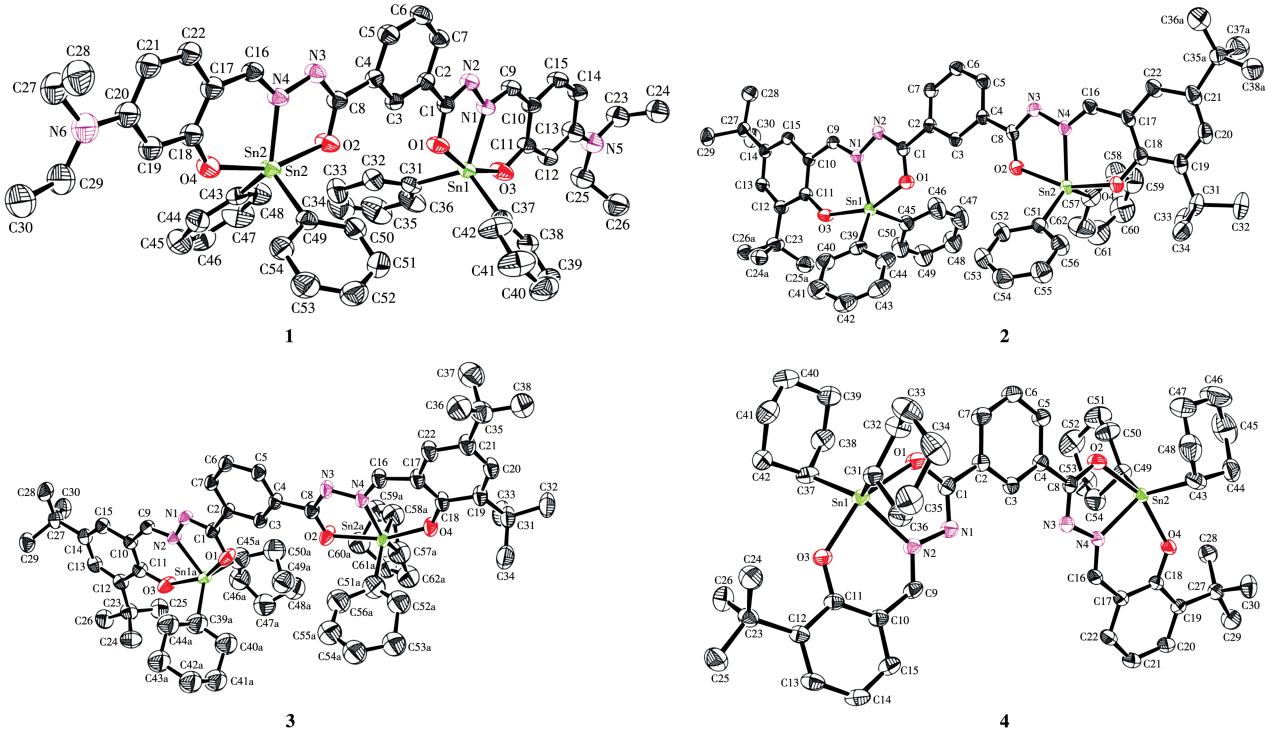

For clarity, H atoms have been omitted, and the disorderly split C atoms (Cb) of **2** and **3** are deleted

Fig.1 Molecular structures of complexes **1-4** with thermal ellipsoids drawn at the 30% probability level

than that of **1** and **2** phenyltin complexes, which further supports the influence of space effect. The bond angle between the equatorial carbon and nitrogen atoms and the axial position, such as ∠O1—Sn1—C(N), varies from 72° to 98°. It can be seen that the central tin and the coordination atom form a distorted triangular bipyramids configuration.

Interestingly, for complexes **1**-**4**, there are some interactions intermolecular in crystal stacking. For example, complex **1** has four $\sigma\cdots\pi$ weak action of adjacent intermolecular: C23—H23A···C32^{i}, C27—H27B···C8^{ii}, C35—H35···C49^{iii}, and C40—H40···C3^{iv} (Symmetry codes: ^{i} 2−x, −y, 1−z; ^{ii} 2−x, 2−y, −z; ^{iii} x, 1+y, −1+z; ^{iv} 1−x, 1−y, −1−z). The distances between the four H···C are 0.286 0, 0.289 5, 0.278 2, and 0.282 6 nm respectively, ∠C—H···C are 146.26°, 127.59°, 153.97°, and 152.96° respectively. A 3D supramolecular structure is formed by these weak interactions.

2.2 Spectral characteristics of the complexes

The infrared spectra of the ligands had four groups of characteristic peaks: (1) 3 400-3 500 cm^{-1} for phenolic hydroxyl group $\nu_{O—H}$ and *ca*. 3 300 cm^{-1} for amino $\nu_{N—H}$ stretching vibration peak; (2) C—H vibrational absorption peaks of the benzene ring (*ca*. 3 000 cm^{-1}) and methyl and methylene (*ca*. 2 800 cm^{-1}); (3) carbonyl (*ca*. 1 700 cm^{-1}, $\nu_{C=O}$) and imine (*ca*. 1 600 cm^{-1}, $\nu_{C=N}$) characteristic peak; (4) benzene C=C vibration absorption peak of the skeleton. There are three groups of chemical shift signals in the NMR spectrum: (1) phenolic hydroxyl hydrogen and amino hydrogen signals appearing at δ=10-13 in the low field region; (2) δ=6-9 for benzene hydrogen (Ar—H) and methylene hydrogen (**H**C=N); (3) δ=1-3 for methyl and methylene hydrogen proton signals in high field. After phenyltin or cyclohexyltin is coordinated with the ligands, the characteristic infrared absorption peak of the phenolic hydroxyl group $\nu_{O—H}$ and amino $\nu_{N—H}$, and its NMR proton signal disappeared in the spectra of the complexes, and the weak peaks of O(N)→Sn and C—Sn[23-24] appeared in the low wavenumber region of the infrared spectrum of the complexes, indicating that the dehydrogenated ligand is coordinated with tin. The stretching peaks of the carbonyl group and the imine group of the ligands shifted towards the low wavenumber in the spectra of complexes, due to the carbonyl enol conversion and Schiff base imine coordination to tin weakening carbonyl and imine groups. After the ligands are coordinated to tin, the electron transfer occurs, and the characteristic lines of the ^{13}C NMR spectra of the complexes shift to the low field region and divide into more lines. In the ^{119}Sn NMR spectra, the chemical shifts of the complexes moved to *ca*. 330 (**1**, **2**) and *ca*. 250 (**3**, **4**) in the high field relative to $SnMe_4$[25], which further indicates that the ligands coordinate with tin as an electron donor.

2.3 Fluorescence properties of ligands and their complexes

The ligands H_4L^1, H_4L^2, and the complexes (**1**-**4**)-chloroform solution with 50 μmol·L^{-1} were prepared. The solution was scanned in 3D on a fluorescence spectrometer and the excitation wavelength of the test solution was determined by referring to the UV spectrum. Then, the fluorescence spectrum of the solution was measured in a range of 400-800 nm at room temperature with 430 nm (H_4L^1), 290 nm (H_4L^2), 370 nm (**1**), 436 nm (**2**), 330 nm (**3**), and 330 nm (**4**) as excitation wavelengths respectively. The results are shown in Fig.2. The H_4L^1-chloroform solution emitted weak fluorescence at 466 nm (*I*=282.2) and 494 nm (*I*=201.7). When complex **1** was formed by H_4L^1 and diphenyltin, the 466 nm peak red-shifted to 476 nm and emitted strong yellow fluorescence. The intensity was 6 037, which was 21.4 times higher than that of H_4L^1; The strong fluorescence of complex-chloroform solution was 34.1 times higher than that of H_4L^1 solution at 494 nm. No fluorescence was found in the H_4L^2-chloroform solution in a range of 400-800 nm. When coordinated with diphenyltin or dicyclohexyltin, complexes **2**- and **3**-chloroform solution produced strong fluorescence at 504 nm, and the fluorescence of solution **3** was 1.3 times that of solution **2**. The luminescence property of complex **4** was similar to that of **3**, with strong fluorescence at 490 nm. It can be seen that the ligand coordinates with diphenyl (dicyclohexyl)tin to form a planar conjugate rigid structure, which greatly increases the fluorescence intensity of the complex compared with

the ligand[26]. Especially when the benzene ring of salicylaldehyde contains color enhancers such as the diethylamine group, the complex produces strong fluorescence and becomes a substance with luminescent properties, which can be further studied as luminescent materials.

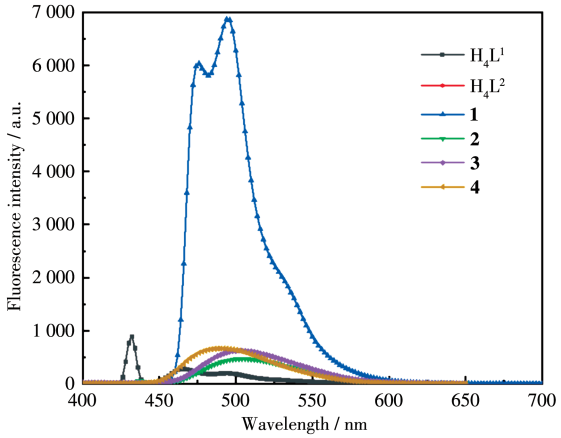

Fig.2 Fluorescence spectra of H_4L^1, H_4L^2, and their complexes **1**-**4** in $CHCl_3$ solution

3 Conclusions

The *m*-phthaloyl bis(substituted salicylaldehyde hydrazone) was prepared by reaction of substituted salicylaldehyde with *m*-phthaloyl hydrazine. *m*-phthaloyl bis(substituted salicylaldehyde hydrazone) tetraphenyl (tetracyclohexyl)ditin complexes were successfully synthesized by methanol solvothermal reaction of ligands with phenyl(cyclohexyl)tin hydroxide. In the preliminary test of the fluorescence properties of 50 μmol·L^{-1} ligands, the complexes-chloroform solution shows that when the ligands with weak fluorescence (H_4L^1) and non-fluorescence (H_4L^2) coordinated with phenyl(cyclohexyl)tin, the chloroform solution of the complexes emitted strong fluorescence, which can be further studied as fluorescent materials.

References:

[1]Gao H, Li J Q, Kang P W, Chigan J Z, Wang H, Liu L, Xu Y S, Zhai L, Yang K W. N-acylhydrazones Confer Inhibitory Efficacy against New Delhi Metallo-β-Lactamase-1. *Bioorg. Chem.*, **2021**,**114**:105138-105138

[2]Yao X D, Hu H M, Wang S B, Zhao W H, Song M X, Zhou Q G. Synthesis, Antimicrobial Activity, and Molecular Docking Studies of Aminoguanidine Derivatives Containing an Acylhydrazone Moiety. *Iran. J. Pharm. Res.*, **2021**,**2021**(2):536-545

[3]Wu S T, Liang X, Luo F, Liu H, Shen L Y, Yang X J, Huang Y, Xu H, Wu N, Zhang Q L, Redshaw C. Synthesis, Crystal Structure and Bioactivity of Phenazine-1-Carboxylic Acylhydrazone Derivatives. *Molecules*, **2021**,**26**(17):5320-5320

[4]Wanderson C S, Lucas D D, Jaqueline E Q, Hérika D A V, Vinícius B S, Andréia M L, Carlos H T P S, Giuliana M V V, Gilberto L B A. Synthesis and *In Silico* Studies of *N*-Acylhydrazone Derivatives as hnRNP K Ligands with Potential Anti-cancer Activity. *Curr. Bioact. Compd.*, **2020**,**16**(4):432-441

[5]Liu Y Y, Peng Q C, Li Y Y, Hou H W, Li K. A Simple Strategy for Constructing Acylhydrazone Photochromic System with Visible Color/Emission Change and Its Application in Photo-Patterning. *Chin. Chem. Lett.*, **2020**,**31**(12):3271-3275

[6]Huang M L, Qiu R X, Pan Z H, Tian D, Tao Y W, Lin J Q, Luo G G. Thermally Triggered Isomerization in a Naphthalene-Based Acylhydrazone with Solid-State Optical Nonlinearity Response. *Eur. J. Inorg. Chem.*, **2020**,**2020**(45):4313-4317

[7]Yang Z Y, Wu D Q, Dai K, Cao S Q, Li Z C, Huang H Y, Shang Z B, Liang H, Yan M H, Xie S Y. A Facile Accessible Acylhydrazone as Al^{3+} Sensor with Excellent Sensitivity and Selectivity. *J. Mol. Struct.*, **2020**,**1201**:1-8

[8]Feng X S, Li X Z, Hu S J, Yan D N, Zhou L P, Sun Q F. Base- and Metal-Dependent Self-Assembly of Lathanide-Organic Coordination Polymers or Macrocycles with Tetradentate Acylhydrazone-Based Ditopic Ligands. *Chem. Asian J.*, **2021**,**16**(11):1392-1397

[9]Popov L D, Levchenkov S I, Lukov V V, Gishko K B, Borodkin S A, Tupolova Y P, Askalepova O I, Vlasenko V G, Spiridonova D V, Lazarenko D A, Burlov A S, Shcherbakov I N. Acylhydrazone Based on 2-*N*-Tosylaminobenzaldehyde and Girard T Reagent: Synthesis, Structure, and Coordination Ability. *Russ. J. Gen. Chem.*, **2021**,**91**(1):90-97

[10]蒲小华. 2-[(*E*)-(3-氯苯胺基)甲基]-6-溴4-氯苯酚Schiff碱的铜及锌的配合物的合成及晶体结构. 无机化学学报, **2012**,**28**(10):2211-2216
PU X H. Synthesis and Crystal Structure of Copper(Ⅱ) and Zinc(Ⅱ) Complexes with Schiff Base 2-((*E*)-(3-Chlorophenylimino)methyl)-6-bromo-4-chlorophenol. *Chinese J. Inorg. Chem.*, **2012**,**28**(10):2211-2216

[11]Luo W, Meng X G, Cheng G Z, Ji Z P. Synthesis, Characterization and Bioactivity of Two Novel Trinuclear Copper(Ⅱ)/Ni(Ⅱ) Complexes with Pentantate Ligand *N*-2-Methyl-acryl-salicylhydrazide. *Inorg. Chim. Acta*, **2009**,**362**:551-555

[12]Gupta P, Panda T, Allu S, Borah S, Baishya A, Gunnam A, Nangia A, Naumov P, Nath N K. Crystalline Acylhydrazone Photoswitches with Multiple Mechanical Responses. *Cryst. Growth. Des.*, **2019**,**19**(5):3039-3044

[13]Chakraborty S, Bhattacharjee C R, Mondal P, Prasad S K, Rao D S S. Synthesis and Aggregation Behaviour of Luminescent Mesomorphic Zinc(Ⅱ) Complexes with 'Salen' Type Asymmetric Schiff Base Ligands. *Dalton Trans.*, **2015**,**44**(16):7477-7488

[14]Maria P, Georgia K M, Maria V. Photo- and Acid-Degradable Polyacylhydrazone-Doxorubicin Conjugates. *Polymers*, **2021**,**13**(15):2461

[15]Lin Z H, Emge T J, Warmuth R. Multicomponent Assembly of Cavitand-Based Polyacylhydrazone Nanocapsules. *Chem. Eur. J.*, **2011**,**17**(34):9395-9405

[16]Terrence J C, Brian G F, Zheng G H, Kimberly L K, Eckard M, Clifford E F R, Wright L J. High Valent Transition Metal Chemistry. Synthesis and Characterization of an Intermediate-Spin Iron(Ⅳ) Complex of a Strong π-Acid Ligand. *J. Am. Chem. Soc.*, **1992**,**114**(22):8724-8725

[17]Liu J J, Liu X R, Zhao S S, Yang Z W, Yang Z. Syntheses, Crystal Structures, Thermal Stabilities, CT-DNA, and BSA Binding Characteristics of a New Acylhydrazone and Its Co(Ⅱ), Cu(Ⅱ), and Zn(Ⅱ) Complexes. *J. Coord. Chem.*, **2020**,**73**(7):1159-1176

[18]Dolomanov O V, Bourhis L J, Gildea R J, Howard J A K, Puschmann H. OLEX2: A Complete Structure Solution, Refinement and Analysis Program. *J. Appl. Cryst.*, **2009**,**42**:339-341

[19]Sheldrick G M. SHELXT-Integrated Space-Group and Crystal-Structure Determination. *Acta Crystallogr. Sect. A*, **2015**,**A71**:3-8

[20]Wu L M, Li Q, Jin L F, Zhou Z Q. Synthesis and Structure of the Acylhydrazone Schiff Base. *Chin. J. Struct. Chem.*, **2010**,**29**(9):1399-1403

[21]Lin H W. Synthesis and Crystal Structure of Isonicotinic Acid [1-(3,5-Dibromo-2-hydroxyphenyl)methylidene]hydrazide Methanol. *Chin. J. Struct. Chem.*, **2007**,**26**(7):773-776

[22]Feng Y L, Zhang F X, Kuang D Z, Yang C L. Two Novel Dibutyltin Complexes with Trimers and Hexanuclear Based on the Bis(5-Cl/Mesalicylaldehyde) Carbohydrazide: Syntheses, Structures, Fluorescent Properties and Herbicidal Activity. *Chin. J. Struct. Chem.*, **2020**,**39**(4):682-692

[23]Nath M, Saini P K. Chemistry and Applications of Organotin(Ⅳ) Complexes of Schiff Bases. *Dalton Trans.*, **2011**,**40**:7077-7121

[24]Yan F F, Ma C L, Li Q L, Zhang S L, Ru J, Cheng S, Zhang R F. Syntheses, Structures and Anti-tumor Activity of Four Organotin(Ⅳ) Dicarboxylates Based on (1,3,4-Thiadiazole-2,5-diyldithio) Diacetic Acid. *New J. Chem.*, **2018**,**42**:11601-11609

[25]Jiang W J, Mo T Z, Zhang F X, Kuang D Z, Tan Y X. Syntheses, Crystal Structures and *In Vitro* Anticancer Activities of Dibenzyltin Compounds Based on the *N*-(2-Phenylacetic acid)-aroyl Hydrazone. *Chin. J. Struct. Chem.*, **2020**,**39**(4):673-681

[26]冯泳兰, 杨春林, 张复兴, 邝代治. 双(取代水杨醛)缩卡巴肼及其苄基锡配合物的合成、表征、荧光性质和除草活性. 无机化学学报, **2019**,**35**(10):1737-1745
FENG Y L, YANG C L, ZHANG F X, KUANG D Z. Synthesis, Characterization, Fluorescence Properties and Herbicidal Activity of Bis(substituted salicylaldehyde) Carbohydrazide and Its Benzyltin Complexes. *Chinese J. Inorg. Chem.*, **2019**,**35**(10):1737-1745